



Radiocarbon analysis  
of elemental and  
organic carbon in  
Switzerland from  
2008–2012 – Part 1

P. Zotter et al.

# Radiocarbon analysis of elemental and organic carbon in Switzerland during winter-smog episodes from 2008 to 2012 – Part 1: Source apportionment and spatial variability

P. Zotter<sup>1</sup>, V. G. Ciobanu<sup>1,\*</sup>, Y. L. Zhang<sup>1,2,3,4</sup>, I. El-Haddad<sup>1</sup>, M. Macchia<sup>5</sup>,  
K. R. Daellenbach<sup>1</sup>, G. A. Salazar<sup>2,3</sup>, R.-J. Huang<sup>1</sup>, L. Wacker<sup>6</sup>, C. Hueglin<sup>7</sup>,  
A. Piazzalunga<sup>8</sup>, P. Fermo<sup>9</sup>, M. Schwikowski<sup>2,3,4</sup>, U. Baltensperger<sup>1</sup>, S. Szidat<sup>2,3</sup>,  
and A. S. H. Prévôt<sup>1</sup>

<sup>1</sup>Laboratory of Atmospheric Chemistry, Paul Scherrer Institute (PSI), 5232 Villigen PSI, Switzerland

<sup>2</sup>Department of Chemistry and Biochemistry, University of Bern, Bern, Switzerland

<sup>3</sup>Oeschger Centre for Climate Change Research, University of Bern, Bern, Switzerland

<sup>4</sup>Laboratory of Radiochemistry and Environmental Chemistry, Paul Scherrer Institute (PSI), 5232 Villigen PSI, Switzerland

<sup>5</sup>CEDAD-Department of Engineering for Innovation, University of Salento, Lecce, Italy

Title Page

Abstract

Introduction

Conclusions

References

Tables

Figures

◀

▶

◀

▶

Back

Close

Full Screen / Esc

Printer-friendly Version

Interactive Discussion



<sup>6</sup>Laboratory of Ion Beam Physics, ETH Höggerberg, Zürich, Switzerland

<sup>7</sup>Laboratory for Air Pollution and Environmental Technology, Swiss Federal Laboratories for Materials Science and Technology (Empa), Überlandstrasse 129, 8600 Dübendorf, Switzerland

<sup>8</sup>University of Milano Bicocca, Department of Earth and Environmental Sciences, 20126 Milano, Italy

<sup>9</sup>Department of Chemistry, University of Milano, 20133 Milano, Italy

\* now at: Centre for Ice and Climate, Niels Bohr Institute, University of Copenhagen, Copenhagen, Denmark

Received: 6 May 2014 – Accepted: 21 May 2014 – Published: 13 June 2014

Correspondence to: A. S. H. Prévôt (andre.prevot@psi.ch)

Published by Copernicus Publications on behalf of the European Geosciences Union.

**Radiocarbon analysis  
of elemental and  
organic carbon in  
Switzerland from  
2008–2012 – Part 1**

P. Zotter et al.

Title Page

Abstract

Introduction

Conclusions

References

Tables

Figures

◀

▶

◀

▶

Back

Close

Full Screen / Esc

Printer-friendly Version

Interactive Discussion

## Abstract

While several studies have investigated winter-time air pollution with a wide range of concentration levels, hardly any results are available for longer time periods covering several winter-smog episodes at various locations; e.g. often only a few weeks from a single winter are investigated. Here, we present source apportionment results of winter-smog episodes from 16 air pollution monitoring stations across Switzerland from five consecutive winters. Radiocarbon ( $^{14}\text{C}$ ) analyses of the elemental (EC) and organic (OC) carbon fractions, as well as levoglucosan, major water-soluble ionic species and gas-phase pollutant measurements were used to characterize the different sources of  $\text{PM}_{10}$ . The most important contributions to  $\text{PM}_{10}$  during winter-smog episodes in Switzerland were on average the secondary inorganic constituents (sum of nitrate, sulfate and ammonium =  $41 \pm 15\%$ ) followed by organic matter OM ( $30 \pm 12\%$ ) and EC ( $5 \pm 2\%$ ). The non-fossil fractions of OC ( $f_{\text{NF,OC}}$ ) ranged on average from 69–85% and 80–95% for stations north and south of the Alps, respectively, showing that traffic contributes on average only up to  $\sim 30\%$  to OC. The non-fossil fraction of EC ( $f_{\text{NF,EC}}$ ), entirely attributable to primary biomass burning, was on average  $42 \pm 13\%$  and  $49 \pm 15\%$  for north and south of the Alps, respectively. While a high correlation was observed between fossil EC and nitrogen oxides, both primarily emitted by traffic, these species did not significantly correlate with fossil OC ( $\text{OC}_\text{F}$ ), which seems to suggest that a considerable amount of  $\text{OC}_\text{F}$  is secondary, formed from fossil precursors. Elevated  $f_{\text{NF,EC}}$  and  $f_{\text{NF,OC}}$  values and the high correlation of the latter with other wood burning markers, including levoglucosan and water soluble potassium ( $\text{K}^+$ ) indicate that biomass burning is the major source of carbonaceous aerosols during winter-smog episodes in Switzerland. The inspection of the non-fossil OC and EC levels and the relation with levoglucosan and water-soluble  $\text{K}^+$  shows different ratios for stations north and south of the Alps, most likely because of differences in burning technologies, for these two regions in Switzerland.

## Radiocarbon analysis of elemental and organic carbon in Switzerland from 2008–2012 – Part 1

P. Zotter et al.

Title Page

Abstract

Introduction

Conclusions

References

Tables

Figures

◀

▶

◀

▶

Back

Close

Full Screen / Esc

Printer-friendly Version

Interactive Discussion



## 1 Introduction

Ambient particulate matter (PM) influences the Earth's climate directly by scattering and absorbing solar radiation and indirectly by modifying cloud microphysics (Pöschl, 2005; IPCC, 2013). In addition, aerosol particles also adversely affect human health as they can cause respiratory and cardiovascular diseases which can lead to increased mortality (Pope and Dockery, 2006; WHO, 2006). In Alpine regions and most parts of Switzerland elevated PM concentrations are often found during winter-time since topography (e.g. alpine valleys) and frequent thermal inversions favor the accumulation of pollutants (Gehrig and Buchmann, 2003; Ruffieux et al., 2006). Environmental pollution control strategies and policies have focused mainly on emissions from fossil fuel combustion so far (e.g. road traffic and industry). However, many recent studies have shown that wood burning emissions from domestic heating can be the dominating source of carbonaceous aerosols during the cold season, in Europe (e.g. Szidat et al., 2006, 2007; Lanz et al., 2008, 2010; Favez et al., 2010; Gilardoni et al., 2011; Harrison et al., 2012; Herich et al., 2014 and references therein). Therefore, the quantification of the fossil and non-fossil, especially wood burning, contributions to PM, particularly for days with high PM concentrations, is crucial for establishing effective mitigation strategies.

Carbonaceous particles are a major fraction of the fine aerosol ( $PM_{2.5}$ ,  $PM < 2.5 \mu m$ ), contributing from 10% up to 90% of the PM mass (Gelencsér, 2004; Putaud et al., 2004; Jimenez et al., 2009). Carbonaceous aerosols are further classified into two sub-fractions: elemental carbon (EC) and organic carbon (OC) (Jacobson et al., 2000). EC originates from incomplete combustion of fossil and non-fossil fuels (e.g. coal, gasoline, diesel, oil and biomass), exclusively emitted directly as primary aerosol in the atmosphere. Meanwhile, OC may be either primary OC (POC) directly emitted in the atmosphere or secondary OC (SOC) formed in the atmosphere through the oxidation of volatile organic compounds (VOCs) from both fossil (coal combustion, industrial and vehicle emissions) and non-fossil (e.g. biomass burning and biogenic

### Radiocarbon analysis of elemental and organic carbon in Switzerland from 2008–2012 – Part 1

P. Zotter et al.

Title Page

Abstract

Introduction

Conclusions

References

Tables

Figures



Back

Close

Full Screen / Esc

Printer-friendly Version

Interactive Discussion







**Radiocarbon analysis  
of elemental and  
organic carbon in  
Switzerland from  
2008–2012 – Part 1**

P. Zotter et al.

Title Page

Abstract

Introduction

Conclusions

References

Tables

Figures

◀

▶

◀

▶

Back

Close

Full Screen / Esc

Printer-friendly Version

Interactive Discussion

These include stations at the Swiss/Italian border where the terrain is more open (e.g. station CHI), plus other stations enclosed within narrow valleys (e.g. stations SVI and ROV). The locations of the stations are shown in Fig. 1 and related details are listed in Table 1. Furthermore, the selection of the stations was also carried out such that the full range of different station characteristics (from urban/traffic to rural background, see Table 1) was covered.

At the selected sites, aerosols were collected onto quartz fiber filters (Pallflex 2500QAT-UP) for 24 h on a regular basis (every 2nd or 4th day or daily depending on the station) using high-volume samplers (Digitel DHA-80, Switzerland) operating at a flow rate of  $500 \text{ L min}^{-1}$  and equipped with  $\text{PM}_{10}$  inlets. After the sampling, filters were wrapped in aluminum foil or lint free paper, sealed in plastic bags, and stored at  $-20^\circ\text{C}$  until analysis. Filter sampling has been widely used but well-known non-systematic artefacts due to adsorption and volatilization of semi-volatile compounds exist (Viana et al., 2006; Jacobson et al., 2000). Since a more complex sampling (e.g. using 2 sampling lines in parallel, one with and the other without a denuder system for volatile OC removal or using 2 filters in series) is not carried out at regular air pollution monitoring stations, artefacts could not be quantified. However, due to the high filter loadings in winter such sampling artefacts are not expected to be large and we assume that they will not significantly influence the results presented in this study. It should be noted that on some filters  $\text{PM}_{10}$  mass was measured gravimetrically which includes weighting before and after the sampling at a relative humidity (RH) of  $50 \pm 2\%$  and a temperature ( $T$ ) of  $20 \pm 2^\circ\text{C}$  after conditioning for 48 h. Since these handling steps may introduce additional artefacts and none of the samples were pre-heated to remove any OC or EC present on the filters prior to sampling, the analysis of blank filters which were treated exactly the same way as the samples is very important. Therefore,  $\sim 50$  field blank filters were collected and 34 of them were analyzed for  $^{14}\text{C}$  in TC, 45 for major water-soluble ionic species and 47 for OC and EC mass loading.

Every winter, five days with high  $\text{PM}_{10}$  concentrations were investigated and therefore, most of the results presented below are considered as representative for winter-





as those used in the THEODORE protocol. The evolving CO<sub>2</sub>, from the THEODORE and the Sunset analyzer, was separated from interfering reaction gases, cryo-trapped and sealed in glass ampoules for <sup>14</sup>C measurements.

The separation of EC for the <sup>14</sup>C measurement was carried out following the Swiss 4S protocol as described by Zhang et al. (2012). First, water-soluble OC (WSOC) and other water-soluble components were removed by water extraction in order to minimize positive artefacts from OC charring (Piazzalunga et al., 2011b; Zhang et al., 2012). The remaining water-insoluble OC (WINSOC) was then removed by a thermal treatment in three steps. In the first two steps, OC was oxidized in O<sub>2</sub> at 375 °C for 150 s and then at 475 °C for 180 s. In the third step, OC was then evaporated in an inert atmosphere in helium at 450 °C for 180 s followed by 180 s at 650 °C. In the end (step four), EC was isolated by the combustion of the remaining carbonaceous material at 760 °C for 150 s in O<sub>2</sub>. This method was optimized to reduce biases in <sup>14</sup>C measurements of EC related to OC charring (leading to higher non-fossil EC (EC<sub>NF</sub>) values) or losses of the least refractory EC (mostly from wood burning) during the WINSOC removal (in the steps one to three) as those would lead to lower EC<sub>NF</sub> fractions. Furthermore, using the Sunset analyzer for the combustion made it possible to quantify those artefacts online, since this instrument monitors the filters during the combustion with a laser. As proposed by Zhang et al. (2012) we tested the effect of different temperatures in step two and three of the thermal protocol on the EC yields and the OC charring for some samples from stations with contrasting sources and filter loadings (e.g. highly and low loaded filters from stations with a large wood burning contribution vs. more traffic influenced stations). Charring of OC most likely occurred only at lower temperature in the steps one and two and was quantified as the difference of the maximum attenuation (ATN) and the initial ATN normalized to the initial ATN of the given thermal step. The EC yield denotes the fraction of EC remaining on the filter samples after the first three OC removal steps before the last step (step four) starts, which was used for the EC recovery for <sup>14</sup>C analysis, and is defined as ratio between the initial ATN of the laser signal through the filter before step one of the thermal treatment and the ATN before

## Radiocarbon analysis of elemental and organic carbon in Switzerland from 2008–2012 – Part 1

P. Zotter et al.

Title Page

Abstract

Introduction

Conclusions

References

Tables

Figures

◀

▶

◀

▶

Back

Close

Full Screen / Esc

Printer-friendly Version

Interactive Discussion





## Radiocarbon analysis of elemental and organic carbon in Switzerland from 2008–2012 – Part 1

P. Zotter et al.

1. *Blank correction.* A mass-dependent blank correction is applied to the measured  $f_M$  values following an isotopic mass balance approach (Zapf et al., 2013):

$$f_{M,\text{corr}} = (mC_{\text{sample}} \times f_{M,\text{sample}} - mC_{\text{blk}} \times f_{M,\text{blk}}) / (mC_{\text{sample}} - mC_{\text{blk}}) \quad (1)$$

where  $f_{M,\text{corr}}$  is the blank corrected  $f_M$ , and  $f_{M,\text{sample}}$  and  $f_{M,\text{blk}}$  are the  $f_M$  measured for samples and blanks, respectively.  $mC_{\text{sample}}$  and  $mC_{\text{blk}}$  denote the carbon mass in the samples and the blanks, respectively. Since blank filters are not available for all stations and years and since the  $^{14}\text{C}$  results of the blanks were not systematically different (between different stations or years, see Fig. S1), the average  $f_M$  and TC values of the blanks,  $0.53 \pm 0.12$  ( $n = 34$ ) and  $2.5 \pm 0.8 \mu\text{g C cm}^{-2}$  ( $n = 47$ ), respectively, were considered for the correction of  $f_{M,\text{OC}}(f_{M,\text{OC},\text{corr}})$ . The blank correction increases the  $f_{M,\text{OC},\text{corr}}$  values by  $\sim 3\%$  and the uncertainty (error propagation of Eq. 1) rises to  $\sim 3\%$ . No EC was detected on the blank filters (see Sect. 2.2 above) and therefore no blank correction was carried out for  $f_{M,\text{EC}}$ .

2. *EC yield correction.* The fraction of EC, which was isolated for the  $^{14}\text{C}$  measurement (EC yield) was on average  $74 \pm 11\%$  as shown in Sect. 2.3.1. However, Zhang et al. (2012) showed that  $f_{M,\text{EC}}$  changes with different EC recoveries. They found a linear relationship between  $f_{M,\text{EC}}$  and the EC yield, which they used to extrapolate  $f_{M,\text{EC}}$  to 100% EC yield using the average slope ( $0.31 \pm 0.1$ ) from several samples ( $n = 5$ ) in order to account for the slight underestimation of biomass burning EC caused by the EC loss during EC isolation for  $^{14}\text{C}$  measurement (see Sect. 2.3.1 above). In this study, we also measured  $f_{M,\text{EC}}$  from 11 samples at different EC yields. As shown in Fig. S2 there is also a linear relationship between the EC yield and  $f_{M,\text{EC}}$  for the samples from this study. Even though the slopes exhibit a larger variability compared to the ones presented in Zhang et al. (2012) the average slope of all winter samples is very similar. In contrast, the slopes for the summer filters show only a very weak relationship between  $f_{M,\text{EC}}$  and the EC yield due to the smaller fraction of less refractory EC (mainly from biomass burning) which is removed before the EC isolation for the  $^{14}\text{C}$  analysis. Beside the

Title Page

Abstract

Introduction

Conclusions

References

Tables

Figures

◀

▶

◀

▶

Back

Close

Full Screen / Esc

Printer-friendly Version

Interactive Discussion



## Radiocarbon analysis of elemental and organic carbon in Switzerland from 2008–2012 – Part 1

P. Zotter et al.

Title Page

Abstract

Introduction

Conclusions

References

Tables

Figures

◀

▶

◀

▶

Back

Close

Full Screen / Esc

Printer-friendly Version

Interactive Discussion



clear difference between samples from summer and winter, no systematic differences between different stations or years were found. Therefore, average slopes of  $0.35 \pm 0.11$  and  $0.07 \pm 0.03$  for winter and summer samples, respectively, were taken to correct all  $f_{M,EC}$  values to 100 % EC yield ( $f_{M,EC,total}$ ) using the following equation (Zhang et al., 2012):

$$f_{M,EC,total} = \text{slope} \times (1 - \text{EC}_{\text{yield}}) + f_{M,EC} \quad (2)$$

The uncertainty of  $f_{M,EC,total}$  was obtained by an error propagation of Eq. (2) using the variability of the average slopes, the measurement uncertainty of  $f_{M,EC}$  and an assigned uncertainty of 10 % for the EC yield and is on average 4.2 %.

3. *Charring correction.* Approximately 50 samples exhibited OC charring contributing > 10 % to EC even though the method used here for EC isolation is optimized to minimize OC charring. Therefore, the  $f_{M,EC,total}$  values were corrected for charring ( $f_{M,EC,final}$ ) using the same isotopic mass balance approach as described in Eq. (1) in which the  $f_M$  and  $mC$  values of the samples and blanks were replaced by  $f_{M,EC,total}$  and EC as well as the amount (formed in step one and two of the thermal treatment as described in Sect. 2.3.1) and  $f_M$  of charred OC ( $f_{M,charr}$ ). We assumed that only 50 % of the charred OC contributed to the  $^{14}C$  result of EC since some charred material was most likely removed in step three. However, since some EC could be lost in step three as well the charred OC evaporated in step three cannot be quantified. Therefore, a high uncertainty of 33 % is assigned to the fraction of charred OC which should in addition account for possible differences and variability between samples and stations. The  $f_{M,charr}$  was obtained from  $^{14}C$  measurements ( $n = 11$ ) of WINSOC from water-extracted filters released in step one and was found to be on average 0.78. To account for possible sample-to-sample differences and variability between samples and stations we assigned an uncertainty of 0.10 for  $f_{M,charr}$ . The uncertainty of  $f_{M,EC,final}$  was on average 4.4 %, which is only slightly higher than for  $f_{M,EC,total}$  (4.2 %).

## Radiocarbon analysis of elemental and organic carbon in Switzerland from 2008–2012 – Part 1

P. Zotter et al.

Title Page

Abstract

Introduction

Conclusions

References

Tables

Figures

◀

▶

◀

▶

Back

Close

Full Screen / Esc

Printer-friendly Version

Interactive Discussion

4. *Bomb peak correction.* Samples from fossil sources are characterized by  $f_M = 0$  due to the extinction of  $^{14}\text{C}$  with a half-life of 5730 years whereas  $f_M$  is equal to one for contemporary carbon sources including biogenic and biomass burning ( $f_{M,\text{bio}}$  and  $f_{M,\text{bb}}$ , respectively). However, due to the thermonuclear weapon tests of the late 1950s and early 1960s the radiocarbon content of the atmosphere increased and  $f_M$  exhibit values greater than one (Levin et al., 2010). To account for this effect, the  $f_{M,\text{OC},\text{corr}}$  and  $f_{M,\text{EC},\text{final}}$  values are converted into non-fossil fractions ( $f_{\text{NF,OC}}$  and  $f_{\text{NF,EC}}$ , respectively) (Szidat et al., 2006; Zhang et al., 2012) using a reference value ( $f_{\text{NF,ref}}$ ) representing the modern  $^{14}\text{C}$  content during the sampling period compared to 1950 before the bomb testing. EC is only emitted from fossil sources or biomass burning. Hence,  $f_{\text{N,ref}}$  equals  $f_{M,\text{bb}}$  to correct  $f_{M,\text{EC}}$  whereas it includes additionally  $f_{M,\text{bio}}$  and the fraction of biogenic sources to the total non-fossil sources ( $\rho_{\text{bio}}$ ) for the calculation of  $f_{\text{NF,OC}} \cdot f_{M,\text{bio}}$  was taken from long-term  $^{14}\text{CO}_2$  measurements at the background station Schauinsland (Levin et al., 2010) and  $f_{M,\text{bb}}$  was estimated using a tree growth model as described in Mohn et al. (2008).  $\rho_{\text{bio}}$  was set to  $0.2 \pm 0.2$  since no large contributions from biogenic sources are expected in Switzerland during winter-smog episodes. In any case,  $\rho_{\text{bio}}$  has only a very little impact on  $f_{\text{NF,ref}}$  compared to other measurement uncertainties (e.g. an increase of  $\rho_{\text{bio}}$  from 0.2 to 0.4 would change  $f_{\text{NF,ref}}$  for this study only by max. 1.8%). The  $f_{M,\text{bio}}$ ,  $f_{M,\text{bb}}$  and  $f_{\text{NF,ref}}$  values for the different years, which were consequently used to determine  $f_{\text{NF,OC}}$  and  $f_{\text{NF,EC}}$ , are shown in Table S3. The final uncertainties for  $f_{\text{NF,OC}}$  and  $f_{\text{NF,EC}}$  ( $\sim 3\%$  and  $\sim 5\%$ , respectively) were derived from an error propagation and include all the individual uncertainties of the  $f_M$  values,  $f_{M,\text{bio}}$ ,  $f_{M,\text{bb}}$  and  $\rho_{\text{bio}}$ .

### 2.4 Analyses of water-soluble major ionic species and levoglucosan

The concentrations of major water-soluble ionic species (cations:  $\text{K}^+$ ,  $\text{Na}^+$ ,  $\text{Mg}^{2+}$ ,  $\text{Ca}^{2+}$  and  $\text{NH}_4^+$ ; anions: methanesulfonate (MSA), oxalate ( $\text{Ox}^{2-}$ ),  $\text{SO}_4^{2-}$ ,  $\text{NO}_3^-$  and  $\text{Cl}^-$ ) were

**Radiocarbon analysis  
of elemental and  
organic carbon in  
Switzerland from  
2008–2012 – Part 1**

P. Zotter et al.

Title Page

Abstract

Introduction

Conclusions

References

Tables

Figures

◀

▶

◀

▶

Back

Close

Full Screen / Esc

Printer-friendly Version

Interactive Discussion

analyzed on all filters ( $n = 320$ ) and field blanks ( $n = 45$ ) with an ion chromatographic system (850 Professional, Metrohm, Switzerland) equipped with a Metrosept C4 cation column and a Metrosept A anion column, respectively. Prior to the measurement a water extraction (15 mL and 50 mL for samples from 2008–2010 and 2011–2012, respectively) with ultrapure water ( $18.2 \text{ M}\Omega \text{ cm}^{-1}$ ) for 30 min at  $40^\circ \text{C}$  in an ultrasonic bath of filter punches with a diameter of 11 mm was carried out. The measurement uncertainty for most of the water-soluble ions was estimated to be 10%. An uncertainty of 30% was assigned for all cations as well as for  $\text{Ox}^{2-}$  and  $\text{Cl}^-$  with concentrations  $< 5$  ppb in solution. A blank correction was carried out subtracting an average value of each ionic species from the concentrations in the samples. In contrast to the blank correction of the OC and TC concentrations as well as  $f_{\text{NF,OC}}$ , where an average value of all blanks (different stations and years) was used, the average of all blanks from the different stations from each winter was taken separately. It should be noted here that not all ionic species were detected in all blanks (see Fig. S1 and Table S2). The overall uncertainty of the major water-soluble ionic species was derived from the error propagation of the measurement uncertainty and the blank variability.

Levoglucosan was measured following the procedures described in Piazzalunga et al. (2010) and (2013a). In brief, levoglucosan was measured by a high-performance anion-exchange chromatography (HPAEC) with pulsed amperometric detection (PAD) using an ion chromatograph (Dionex ICS1000) equipped with an isocratic pump and a sample injection valve with a  $100 \mu\text{L}$  sample loop. Prior to the analysis, a water extraction was carried out by three subsequent extractions of  $\sim 2 \text{ cm}^2$  filter punches by 20 min sonication using 2 mL Millipore-MilliQ water ( $18.2 \text{ M}\Omega \text{ cm}^{-1}$ ). Levoglucosan was then separated from other compounds by a CarboPac PA-10 guard column ( $50 \text{ mm} \times 4 \text{ mm}$ ) and a CarboPac PA-10 anion exchange analytical column ( $250 \text{ mm} \times 4 \text{ mm}$ ) using 18 mM NaOH as an eluent. The analytical system comprised an amperometric detector (Dionex ED50) equipped with an electrochemical cell. The detector cell had a disposable gold electrode and a pH electrode as reference (both from Dionex) and was operated in the pulsed amperometric detection (PAD) mode. The measurement uncer-

tainty was estimated to be  $\sim 5\%$  using the average repeatability of several standards and the limit of detection in solution is 2 ppb. The levoglucosan concentrations were also analyzed for blank filters but were below the detection limit and therefore no blank correction was performed.

## 2.5 Additional data

Since all sampling sites in this project are part of the Swiss national (NABEL) or cantonal air pollution monitoring networks, additional parameters (e.g. gas phase pollutants, particle mass and meteorology) are routinely measured. PM<sub>10</sub> and nitrogen oxides (NO<sub>x</sub> = NO and NO<sub>2</sub>) data are available from all stations (except SCH), whereas ozone (O<sub>3</sub>), sulfur dioxide (SO<sub>2</sub>) and carbon monoxide (CO) measurements are only performed at some stations. Reference instrumentation according to the valid European standards was used. It should be noted that NO<sub>x</sub> measurements using molybdenum converters suffer from interference of oxidation products of NO<sub>x</sub> which is however not crucial for winter-time conditions (Steinbacher et al., 2007). The meteorological parameters wind-speed, wind-direction, temperature (*T*), relative humidity (RH), precipitation and global radiation were also only measured at some of the sites. For the remaining sampling locations meteorological data were taken from nearby stations operated by the Swiss weather service (MeteoSwiss, 2014). In all networks (NABEL, Cantons and MeteoSwiss) data sets undergo an automatic and a manual quality check (data should be (1) within a plausible range, (2) show plausible variability, (3) reproduce to a reasonable extent the expected daily, monthly and yearly variations, (4) whenever possible measurements are compared to nearby or similar stations with the expectation of similar values, Barmpadimos et al., 2011).

## Radiocarbon analysis of elemental and organic carbon in Switzerland from 2008–2012 – Part 1

P. Zotter et al.

Title Page

Abstract

Introduction

Conclusions

References

Tables

Figures

◀

▶

◀

▶

Back

Close

Full Screen / Esc

Printer-friendly Version

Interactive Discussion



## 3 Results and discussion

### 3.1 Composition of PM<sub>10</sub>

One aim of this study was the source apportionment of winter smog episodes in Switzerland. As explained above only days with high PM<sub>10</sub> concentrations at all stations were analyzed. As shown in Fig. 2a the selected days from almost all locations fulfilled on average this criterion. While not exactly the same days were chosen for stations north and south of the main chain of the Alps, it is nevertheless evident that the PM<sub>10</sub> burden during winter-smog episodes in Switzerland is higher south of the Alps ( $73 \pm 27 \mu\text{g m}^{-3}$  in the south compared to  $55 \pm 16 \mu\text{g m}^{-3}$  in the north). These episodes often occur in winter during stable meteorological conditions including periods with high pressure, rather low temperatures and weak winds (typically less than  $2 \text{ m s}^{-1}$ ). Such conditions often lead to inversions with low mixing layer heights, thereby favoring the accumulation of pollutants and consequently causing high PM<sub>10</sub> concentrations. The reason for the higher PM<sub>10</sub> values at stations south of the Alps is most likely due to a combination of topography (e.g. several stations are located in alpine valleys), local meteorology (e.g. more persistent inversions with rather low mixing heights compared to the north) and emissions (strong local wood burning influence, see Sects. 3.2.1 and 3.2.2 below).

As only five winter-smog-episode days from each of the five winter seasons were selected and to account for possible differences in the concentration levels between the stations (especially locations north vs. south of the Alps), we will mainly focus here on the fractional contributions of the individual compounds to total PM<sub>10</sub>. The major water-soluble ions, EC and OM measured here explain  $79 \pm 10\%$  of the total PM<sub>10</sub> mass. The missing fraction could mostly be attributed to aerosol water content, the water insoluble fraction (e.g., dust particles), and/or to the uncertainties of the different measurement methods and OM:OC ratio used to convert OC to OM. The major contributors to PM<sub>10</sub> during winter-smog episodes in Switzerland were on average the

## Radiocarbon analysis of elemental and organic carbon in Switzerland from 2008–2012 – Part 1

P. Zotter et al.

Title Page

Abstract

Introduction

Conclusions

References

Tables

Figures

◀

▶

◀

▶

Back

Close

Full Screen / Esc

Printer-friendly Version

Interactive Discussion



for the stations south of the Alps. The relative contributions of  $\text{NO}_3^-$  and  $\text{NH}_4^+$  exhibit a trend towards lower values at rural stations, as opposed to the OM fraction (see Fig. 2), which may be due to the influence of the stations in the south by air masses advected from the Po Valley, where emissions from fossil fuel combustion (e.g.  $\text{NO}_x$ ) are elevated (Piazzalunga et al., 2011a; Larsen et al., 2012) compared to the southern part of Switzerland. More details about the influence of air masses originating from other regions outside Switzerland will be discussed Zotter et al. (2014).

## 3.2 $^{14}\text{C}$ -based source apportionment

### 3.2.1 Relative fossil and non-fossil contributions of OC and EC

Figure 3 summarizes the individual results of all  $^{14}\text{C}$  measurements ( $n \sim 300$  for OC and EC) from all stations for the five winters (2007/2008–2011/2012), except for REI, MOL, ROV and SCH (one winter) and BAS (two winters), as noted in Table 2. The use of Whisker boxplots enables the identification of the variability of the results for each station as well as the station-to-station differences. Several filters from BAS showed clearly elevated  $f_{\text{NF,OC}}$  values (larger than one and up to five) indicating that BAS is influenced by sources emitting anthropogenic  $^{14}\text{C}$  (e.g. from nuclear power plants, pharmaceutical industry and biochemical laboratories working with labeled  $^{14}\text{C}$ , incinerators for medical waste). BAS is the base for two of the world's largest pharmaceutical enterprises, Roche and Novartis, and in addition an incinerator for medical waste is located in the vicinity of the station. Furthermore,  $^{14}\text{C}$  measurements on leaf samples across the city of Basel also showed partially highly elevated results (BAG, 2008), indicating  $^{14}\text{C}$ -enriched  $\text{CO}_2$ . Therefore,  $f_{\text{NF,OC}}$  values from BAS were not considered for the further analysis. This artefact is however restricted to OC; the  $f_{\text{NF,EC}}$  results did not show such an influence (see Fig. 3b) and are included and discussed throughout this study. The data from the yearly cycle in ZUR is also excluded here but will be investigated in part II (Zotter et al., 2014).

## Radiocarbon analysis of elemental and organic carbon in Switzerland from 2008–2012 – Part 1

P. Zotter et al.

Title Page

Abstract

Introduction

Conclusions

References

Tables

Figures

◀

▶

◀

▶

Back

Close

Full Screen / Esc

Printer-friendly Version

Interactive Discussion



**Radiocarbon analysis  
of elemental and  
organic carbon in  
Switzerland from  
2008–2012 – Part 1**

P. Zotter et al.

Title Page

Abstract

Introduction

Conclusions

References

Tables

Figures

◀

▶

◀

▶

Back

Close

Full Screen / Esc

Printer-friendly Version

Interactive Discussion

The range of all  $f_{\text{NF,OC}}$  values (except BAS) as displayed in Fig. 3a is 0.59–0.95 and 0.62–1.02 for stations north and south of the Alps, respectively. A few samples ( $n = 4$ ) with  $f_{\text{NF,OC}}$  values slightly above one were found in SVI and are within the uncertainty ( $\sim 3\%$ ) of  $f_{\text{NF,OC}}$ . They can be explained on the one hand with very high local wood-burning contributions and on the other hand with the uncertainties in the reference value  $f_{\text{NF,ref}}$  used for the correction of the still elevated  $^{14}\text{C}$  concentrations due to the above-ground thermo-nuclear bomb tests (see Sect. 2.3.2). The average  $f_{\text{NF,OC}}$  values for stations north and south of the alps are  $0.78 \pm 0.08$  (median = 0.78) and  $0.82 \pm 0.07$  (median = 0.83), respectively, showing that on average locations south of the Alps are more impacted ( $t$  test, significant at 95 %,  $p = 3.4 \times 10^{-12}$ ) by non-fossil sources. As discussed above, non-fossil OC may include, POC and SOC from biomass burning and cooking emissions, as well as primary biological particles and biogenic SOC. Cooking was estimated to contribute on average only 7.5 % to OA during winter in ZUR which is the largest city of Switzerland (Canonaco et al., 2013), and is therefore expected to contribute less at the other stations. Furthermore, large inputs from biological and biogenic sources are also not expected under Swiss winter conditions, characterized by low biological activity. Therefore, the high  $f_{\text{NF,OC}}$  values indicate that wood burning POC and SOC are most probably the main source of OC during winter-smog episodes in Switzerland. The highest  $f_{\text{NF,OC}}$  values north and south of the Alps were found at the rural stations SCH ( $0.85 \pm 0.04$ ) and SVI ( $0.95 \pm 0.05$ ), which are located in narrow alpine valleys. The lowest non-fossil contributions to OC were observed in BER, STG, VAD and ZUR north of the Alps as well as in MOL and CHI south of the Alps, but were on average never below 70 % showing that sources of fossil carbon only account for a small fraction of OC during winter-smog episodes in Switzerland, even at urban and traffic-influenced stations. Furthermore, the variability of all  $f_{\text{NF,OC}}$  values for the individual stations and the station to station differences (with the exception of SVI and BER which present the highest and lowest values, respectively) are low as displayed by the small interquartile ranges (IQR = 3rd–1st quartile;  $0.10 \pm 0.02$  and  $0.08 \pm 0.02$  for stations north and south of the Alps, respectively) and the small range of the station

averages (0.75–0.85 and 0.80–0.86 for stations north and south of the Alps, respectively). This suggests that the relative source contributions to OC are very consistent within Switzerland during winter-smog episodes.

Similar high non-fossil contributions to OC were also found in previous studies in Switzerland. The  $f_{\text{NF,OC}}$  values for ZUR, ROV, MOL, REI and Sedel as well as MAS, Saxon, Sion and Brigerbad ranged on average from 61–76 % with values above 90 % in ROV (Szidat et al., 2006, 2007; Sandradewi et al., 2008a, c; Perron et al., 2010). Results previously reported for other regions in Europe show lower biomass burning contributions to OC. For example the biomass burning OC ( $\text{OC}_{\text{BB}}$ ) to the total OC fraction at three Austrian cities (Vienna, Graz and Salzburg), three locations in the Po Valley (Milan, Sondrio and Ispra) and in Grenoble was found to range from 35–54 % (Caseiro et al., 2009), 28–65 % (Gilardoni et al., 2011; Piazzalunga et al., 2011a) and 60 % (Favez et al., 2010), respectively.

The non-fossil fraction of EC relate more unambiguously to biomass burning. For most stations the wood burning contribution was found to be < 50 % and thus the contribution from fossil fuel combustion, mostly due to traffic, was > 50 % (see Fig. 3b). However, since the average  $f_{\text{NF,EC}}$  values, except for BER, REI and MOL, never decrease below 0.4, it is evident that wood burning emissions exceptionally account for a large fraction of EC during winter-smog episodes in Switzerland. The individual  $f_{\text{NF,EC}}$  values range from 0.12–0.79 (on average  $0.42 \pm 0.13$ ) and 0.25–0.87 (on average  $0.49 \pm 0.15$ ) for all stations north and south of the Alps, respectively, showing that for EC the contributions from biomass burning are higher for locations south of the Alps ( $t$  test, significant at 95 %,  $p = 3.7 \times 10^{-4}$ ). The lowest  $f_{\text{NF,EC}}$  values were found at the stations BER ( $0.22 \pm 0.06$ ), MOL ( $0.28 \pm 0.06$ ) and REI ( $0.35 \pm 0.05$ ), which are directly exposed to traffic emissions from nearby roads with a high traffic flow. Extremely high non-fossil contributions to EC up to 87 % and 79 % were observed in SVI ( $66 \pm 11$  %) and SCH ( $69 \pm 9$  %), respectively. Both stations are located in narrow alpine valleys characterized by frequent winter-time inversions and are strongly influenced by local

## Radiocarbon analysis of elemental and organic carbon in Switzerland from 2008–2012 – Part 1

P. Zotter et al.

Title Page

Abstract

Introduction

Conclusions

References

Tables

Figures

◀

▶

◀

▶

Back

Close

Full Screen / Esc

Printer-friendly Version

Interactive Discussion





shows the average  $EC_F$ ,  $EC_{NF}$ ,  $OC_{NF}$  and  $OC_F$  concentrations as well as their relative contributions to TC for all analyzed winter samples for each station. It is evident that sources of non-fossil carbon dominate TC at locations north and south of the Alps with contributions around  $70 \pm 18\%$  and  $79 \pm 10\%$  (sum of  $EC_{NF}$  and  $OC_{NF}$ ), respectively.

5 Compared to other winter measurements across Europe this is rather at the higher end of the reported range and higher than reported for urban sites around the world but similar to values found for suburban and rural locations in the US and India (Hodzic et al., 2010; Heal, 2014).

$OC_{NF}$  is the largest fraction of TC, accounting on average for  $61 \pm 8\%$  and  $69 \pm 9\%$  for stations north and south of the Alps, respectively, whereas  $EC_{NF}$  contributes on average  $\sim 9\%$  to TC in both regions of Switzerland. The fossil shares of OC and EC are higher north of the Alps ( $18 \pm 6\%$  and  $13 \pm 6\%$  compared to  $12 \pm 6\%$  and  $10 \pm 5\%$  in the south, respectively). The lowest and highest fossil contributions to TC (sum of  $EC_F$  and  $OC_F$ ) were found in SVI ( $10 \pm 6\%$ ) and BER ( $43 \pm 7\%$ ), respectively. For the stations south of the Alps, a clear decreasing trend in the relative contribution of fossil OC and EC from more traffic to more rural influenced stations is found (see Figs. 4 and S4).

10 North of the Alps, such a trend is only evident for  $EC_F$ . Relative and absolute non-fossil OC and EC contributions in the north (except BER and SCH which present the highest and lowest values) only show low station-to-station differences (station averages range from  $58\text{--}71\%$  and  $1.5\text{--}2.5 \mu\text{g C m}^{-3}$  as well as  $8\text{--}11\%$  and  $0.9\text{--}1.9 \mu\text{g C m}^{-3}$  for  $OC_{NF}$  and  $EC_{NF}$ , respectively, see Figs. 4 and S4 in the Supplement). In addition, also the variability of the relative and absolute  $OC_{NF}$  and  $EC_{NF}$  contributions at the individual stations north of the Alps is rather small as evidenced by low IQRs ( $2.8 \pm 0.9 \mu\text{g C m}^{-3}$  and  $7 \pm 2\%$  as well as  $0.4 \pm 0.1 \mu\text{g C m}^{-3}$  and  $3 \pm 1\%$  for  $OC_{NF}$  and  $EC_{NF}$ , respectively).

20 Together with the low station-to-station differences, this suggests on the one hand that non-fossil sources very consistently influence stations on the Swiss Plateau and that the degree of atmospheric processing and SOC formation for the chosen days were very similar and on the other hand that the different stations on the Swiss Plateau are rather influenced by regional (still mainly within Switzerland) air pollution. This is con-

Radiocarbon analysis  
of elemental and  
organic carbon in  
Switzerland from  
2008–2012 – Part 1

P. Zotter et al.

Title Page

Abstract

Introduction

Conclusions

References

Tables

Figures

◀

▶

◀

▶

Back

Close

Full Screen / Esc

Printer-friendly Version

Interactive Discussion



## Radiocarbon analysis of elemental and organic carbon in Switzerland from 2008–2012 – Part 1

P. Zotter et al.

Title Page

Abstract

Introduction

Conclusions

References

Tables

Figures

◀

▶

◀

▶

Back

Close

Full Screen / Esc

Printer-friendly Version

Interactive Discussion

5 firmed by high correlations ( $r = 0.7 \pm 0.2$ ,  $0.5 \pm 0.3$ ,  $0.9 \pm 0.1$  and  $0.7 \pm 0.1$ , respectively) between the concentrations of  $EC_F$ ,  $EC_{NF}$ ,  $OC_F$  and  $OC_{NF}$  for all measured values from each station located on the Swiss Plateau (see Table 1) against ZUR which was chosen as a reference for this region. Furthermore, this is in agreement with Gehrig and

10 Buchmann (2003) who previously found that (1) under high pressure conditions inversions can extend over the entire Swiss Plateau and typically last several days possibly causing smog formation and (2) that PM concentrations were strongly influenced by meteorology (dilution with clean air or precipitation) rather than by variation of source activities. In contrast, correlating the absolute fossil and non-fossil contributions of OC

15 and EC from stations south of the Alps against the ones from MAG shows lower values ( $r = 0.3 \pm 0.2$ ,  $0.6 \pm 0.3$ ,  $0.4 \pm 0.3$  and  $0.3 \pm 0.3$  for  $OC_{NF}$ ,  $EC_{NF}$ ,  $EC_F$  and  $OC_F$ , respectively) indicating that local sources are more important for stations south of the Alps.

### 3.3 Sources and behavior of fossil and non-fossil organic carbon

#### 15 3.3.1 Fossil fraction

Figure 5 presents the comparison between  $EC_F$ ,  $OC_F$  and  $NO_x$ , which are expected to be associated with traffic emissions, in Switzerland.  $EC_F$ , which is emitted as primary aerosol from vehicles, exhibits a high correlation with  $NO_x$  for the stations north ( $r = 0.79$ ) and south ( $r = 0.75$ ) of the Alps, with similar slopes and axis intercepts for both regions ( $0.021$  and  $0.015 \mu\text{g C m}^{-3} \text{ ppb}^{-1}$  and  $0.35$  and  $0.89 \mu\text{g C m}^{-3}$  for north and south of the Alps, respectively, see Fig. 5c), indicating a rather similar fleet composition in the two areas. Similar slopes ( $0.05$ ,  $0.03$  and  $0.02 \mu\text{g C m}^{-3} \text{ ppb}^{-1}$ ) have been reported previously for 3 locations in Switzerland (MAG, ZUR and PAY, Herich et al., 2011), Grenoble (Favez et al., 2010) and London (Liu et al., 2014). In contrast,

20 no correlation is found between  $OC_F$  and the primary vehicular markers,  $EC_F$  and  $NO_x$  ( $r < 0.5$ , see Fig. 5b) for stations both north and south of the Alps. Further, the amounts of fossil organic carbon measured are significantly higher than amounts

expected for traffic emissions; i.e. observed average  $OC_F/EC_F = 1.54 \pm 0.83$  vs. traffic  $OC/EC = 0.25 - 0.80$  (El Haddad et al., 2013 and references therein). Taken together these observations indicate that a considerable amount of  $OC_F$  is associated with emissions or atmospheric pathways that yield organic aerosol with little or no  $EC_F$  and  $NO_x$ .

5 These may include primary emissions from non-mobile fossil fuel combustion sources, e.g. heavy fuel (e.g. crude oil) combustion (not widely used in Switzerland), or secondary organic carbon formed from fossil VOCs emitted from traffic.

### 3.3.2 Non-fossil fraction

As mentioned above a significant fraction of non-fossil carbon during winter-smog episodes originates from biomass burning. The use of a single or a set of source specific compound markers from wood burning emissions is often applied to estimate the contribution of this source to ambient aerosol (Herich et al., 2014 and references therein). The most widely used tracer compound for biomass-burning emissions is levoglucosan (Simoneit et al., 1999; Puxbaum et al., 2007; Viana et al., 2013), a product of cellulose combustion. Another wood burning tracer is water-soluble potassium ( $K^+$ ), which is an inorganic compound mainly present in ash. The wide variability of levoglucosan emission ratios results in significant uncertainties in estimating wood burning contributions. For example, ratios of OC and EC to levoglucosan for alpine regions were reported in Schmidl et al. (2008) to range from 3.7 to 12.5 and from 0.7 to 4.7, respectively, dependent on the combustion conditions and fuel type used (Engling et al., 2006; Lee et al., 2010). Here, we examine the relationship between different measured wood burning markers and the measured  $OC_{NF}$ , to investigate the main emission sources and chemical characteristics of this fraction.

25 The comparison of  $EC_{NF}$  and  $OC_{NF}$  with levoglucosan (see Fig. 6) shows a high correlation for both species with the latter. The small intercept (1.3 and  $2.3 \mu\text{gC m}^{-3}$  for stations north and south of the Alps, respectively) and the high correlation ( $r > 0.87$ ) between  $OC_{NF}$  and levoglucosan suggests that the majority of  $OC_{NF}$  originates from

Radiocarbon analysis  
of elemental and  
organic carbon in  
Switzerland from  
2008–2012 – Part 1

P. Zotter et al.

Title Page

Abstract

Introduction

Conclusions

References

Tables

Figures



Back

Close

Full Screen / Esc

Printer-friendly Version

Interactive Discussion



ence for the years 2008–2012) suggesting that households in both regions have similar access to soft and hard woods. Therefore, the different ratios between  $OC_{NF}$  and  $K^+$  as well as levoglucosan and  $K^+$  are most likely due to different burning conditions. Previous studies demonstrated that particulate emissions from biomass combustion with high temperatures (e.g. in large combustion units, modern stoves and boilers) consist predominantly of inorganic material (K-salts) and contain little OC (Valmari et al., 1998; Johansson et al., 2003; Khalil and Rasmussen, 2003; Heringa et al., 2011; Schmid et al., 2011). Consequently, dissimilar levoglucosan to  $K^+$  ratios measured at different locations have already been used as indication for different burning conditions in recent studies (Sандрadewi et al., 2008c; Caseiro et al., 2009; Piazzalunga et al., 2013b). The lower levoglucosan to  $K^+$  ratios found in this study for locations north of the Alps therefore suggest a larger fraction of more efficient wood burners (e.g. pellet and wood chip burners) in this region compared to the south where wood stoves seem to be operated at rather poor combustion conditions with high carbonaceous and thus lower relative  $K^+$  emissions.

The discussions above clearly showed the differences in wood burning marker ratios at locations north and south of the Alps. However, a closer inspection of the results of Table 3 reveals that most wood burning marker ratios at the stations PAY and MAS (both north of the Alps) are rather similar to the average over all locations south of the Alps and the urban station CHI exhibits values more similar to the average in the north than to the other southern locations. Since in the north mainly urban and suburban stations and south of the Alps mostly rural and/or background sites were chosen (see Table 1 and Fig. 1), this suggests that the differences in the wood burning marker ratios between these two Swiss regions are most likely associated with the different station characteristics (e.g. rural and/or background with high wood burning influence vs. urban, suburban and more traffic influenced stations) rather than due to their geographical location within Switzerland.

## Radiocarbon analysis of elemental and organic carbon in Switzerland from 2008–2012 – Part 1

P. Zotter et al.

Title Page

Abstract

Introduction

Conclusions

References

Tables

Figures

◀

▶

◀

▶

Back

Close

Full Screen / Esc

Printer-friendly Version

Interactive Discussion



### 3.3.3 Comparison of wood burning marker ratios with other studies

Herich et al. (2014) presented an overview about previous studies carried out during winter in Switzerland and other alpine regions in Europe. Several source apportionment methods (including  $^{14}\text{C}$  analysis, aethalometer model, positive matrix factorisation, chemical mass balance, macro tracer approach) were used in these studies to estimate the wood burning fraction of OC and EC. In the following we will compare our biomass burning marker ratios with the ones summarized by Herich et al. (2014). It should be noted that the results presented in the latter study were mainly obtained from short campaigns in just a single winter season and at a limited number of stations, whereas here we performed measurements on winter filters from five years and 16 stations.

The average  $\text{EC}_{\text{NF}}$  to levoglucosan ratio for several stations north of the Alps (BER, PAY, STG, ZUR, REI, BAS, Ebnet-Kappel) from earlier winter measurements in Switzerland is  $1.82 \pm 0.44$ , and is consistent with the results obtained here ( $1.72 \pm 0.59$ , see Table 3).  $\text{EC}_{\text{NF}}$ /levoglucosan for some southern stations (MAG, MOL, ROV) is on average  $1.20 \pm 0.37$ , which is slightly higher than the average ratio found here ( $0.87 \pm 0.27$ , see Table 3).  $\text{EC}_{\text{NF}}$ /levoglucosan ratios for three Austrian cities (1.18–1.38 for Vienna, Graz and Salzburg, Caseiro et al., 2009) and three locations in the Po Valley (0.84–1.16 for Milan, Sondrio and Ispra, Gilardoni et al., 2011; Piazzalunga et al., 2011a) which can be considered as north and south of the main chain of the Alps, respectively, exhibit also similar values as those obtained here. Generally lower biomass burning OC ( $\text{OC}_{\text{BB}}$ ) to levoglucosan and  $\text{OC}_{\text{BB}}$  to  $\text{EC}_{\text{NF}}$  ratios for the Swiss, Po-Valley and Austrian sites located north and south of the Alps were found in Herich et al. (2014) compared to  $\text{OC}_{\text{NF}}$  to levoglucosan and  $\text{OC}_{\text{NF}}$  to  $\text{EC}_{\text{NF}}$  ratios presented here ( $12.6 \pm 3.1$  and  $7.7 \pm 2.1$ , respectively, in the north as well as  $7.81 \pm 2.70$  and  $8.6 \pm 2.9$ , respectively, in the south, see Table 3).  $\text{OC}_{\text{BB}}$  to levoglucosan ratios previously found in the north and south of Switzerland, in Austria and the Po-Valley are  $9.05 \pm 1.77$ ,  $7.04 \pm 0.90$ ,  $7.24 \pm 0.03$  and  $5.62 \pm 0.30$ , respectively, and  $\text{OC}_{\text{BB}}$  to  $\text{EC}_{\text{NF}}$  ratios previously reported





recent studies which have shown that wood burning can be the dominating source of carbonaceous aerosols during the cold season, in Europe.

The comparison between fossil EC ( $EC_F$ , only emitted as primary aerosol) and nitrogen oxides ( $NO_x$ ), which are mainly associated with traffic emissions, showed a good agreement whereas no correlation was observed between fossil OC ( $OC_F$ ) and the two latter components, indicating that a considerable amount of  $OC_F$  is secondary OC (SOC) formed from fossil precursors emitted from traffic. Correlations between non-fossil OC ( $OC_{NF}$ ) and EC ( $EC_{NF}$ ) and the wood burning markers levoglucosan and water soluble potassium ( $K^+$ ) clearly show different slopes for stations north and south of the Alps suggesting different burning technologies in both regions.

**The Supplement related to this article is available online at  
doi:10.5194/acpd-14-15591-2014-supplement.**

*Acknowledgements.* This work was funded by the Swiss Federal Office for the Environment (BAFU), inNet Monitoring AG, OSTLUFT, the country Liechtenstein and the Swiss Cantons Basel-Stadt, Basel-Landschaft, Graubünden, St. Gallen, Solothurn, Valais, Uri and Ticino.

## References

Andersson, A., Sheesley, R. J., Kruså, M., Johansson, C., and Gustafsson, Ö.:  $^{14}C$ -based source assessment of soot aerosols in Stockholm and the Swedish EMEP-Aspvreten regional background site, *Atmos. Environ.*, 45, 215–222, doi:10.1016/j.atmosenv.2010.09.015, 2011.

BAG – Bundesamt für Gesundheit, Jahresberichte Umweltradioaktivität und Strahlendosen: Umweltradioaktivität und Strahlendosen in der Schweiz 2007, available at: <http://www.bag.admin.ch/themen/strahlung/00043/00065/02239/index.html?lang=de> (last access: 30 April 2014), 2008.

**Radiocarbon analysis  
of elemental and  
organic carbon in  
Switzerland from  
2008–2012 – Part 1**

P. Zotter et al.

Title Page

Abstract

Introduction

Conclusions

References

Tables

Figures

◀

▶

◀

▶

Back

Close

Full Screen / Esc

Printer-friendly Version

Interactive Discussion



**Radiocarbon analysis  
of elemental and  
organic carbon in  
Switzerland from  
2008–2012 – Part 1**

P. Zotter et al.

Title Page

Abstract

Introduction

Conclusions

References

Tables

Figures

◀

▶

◀

▶

Back

Close

Full Screen / Esc

Printer-friendly Version

Interactive Discussion

- Barnpadimos, I., Hueglin, C., Keller, J., Henne, S., and Prévôt, A. S. H.: Influence of meteorology on PM<sub>10</sub> trends and variability in Switzerland from 1991 to 2008, *Atmos. Chem. Phys.*, 11, 1813–1835, doi:10.5194/acp-11-1813-2011, 2011.
- Bernardoni, V., Calzolai, G., Chiari, M., Fedi, M., Lucarelli, F., Nava, S., Piazzalunga, A., Riccobono, F., Taccetti, F., Valli, G., and Vecchi, R.: Radiocarbon analysis on organic and elemental carbon in aerosol samples and source apportionment at an urban site in Northern Italy, *J. Aerosol. Sci.*, 56, 88–99, doi:10.1016/j.jaerosci.2012.06.001, 2013.
- Canonaco, F., Crippa, M., Slowik, J. G., Baltensperger, U., and Prévôt, A. S. H.: SoFi, an IGOR-based interface for the efficient use of the generalized multilinear engine (ME-2) for the source apportionment: ME-2 application to aerosol mass spectrometer data, *Atmos. Meas. Tech.*, 6, 3649–3661, doi:10.5194/amt-6-3649-2013, 2013.
- Caseiro, A., Bauer, H., Schmidl, C., Pio, C. A., and Puxbaum, H.: Wood burning impact on PM<sub>10</sub> in three Austrian regions, *Atmos. Environ.*, 43, 2186–2195, doi:10.1016/j.atmosenv.2009.01.012, 2009.
- Cavalli, F., Viana, M., Yttri, K. E., Genberg, J., and Putaud, J.-P.: Toward a standardised thermal-optical protocol for measuring atmospheric organic and elemental carbon: the EUSAAR protocol, *Atmos. Meas. Tech.*, 3, 79–89, doi:10.5194/amt-3-79-2010, 2010.
- Ceburnis, D., Garbaras, A., Szidat, S., Rinaldi, M., Fahrni, S., Perron, N., Wacker, L., Leinert, S., Remeikis, V., Facchini, M. C., Prevot, A. S. H., Jennings, S. G., Ramonet, M., and O'Dowd, C. D.: Quantification of the carbonaceous matter origin in submicron marine aerosol by <sup>13</sup>C and <sup>14</sup>C isotope analysis, *Atmos. Chem. Phys.*, 11, 8593–8606, doi:10.5194/acp-11-8593-2011, 2011.
- Cercl'Air – Schweizerische Gesellschaft der Lufthygiene-Fachleute:, available at: <http://www.cerclair.ch/cmsv2/index.php> (last access: 30 April 2014), 2012.
- Chow, J. C., Watson, J. G., Pritchett, L. C., Pierson, W. R., Frazier, C. A., and Purcell, R. G.: The DRI thermal optical reflectance carbon analysis system – description, evaluation and application in United-States air-quality studies, *Atmos. Environ.*, 27, 1185–1201, doi:10.1016/0960-1686(93)90245-t, 1993.
- Chow, J. C., Watson, J. G., Crow, D., Lowenthal, D. H., and Merrifield, T.: Comparison of IMPROVE and NIOSH carbon measurements, *Aerosol Sci. Tech.*, 34, 23–34, doi:10.1080/027868201300081923, 2001.
- Currie, L. A.: The remarkable metrological history of radiocarbon dating [II], *J. Res. Natl. Inst. Stan.*, 109, 185–217, doi:10.6028/jres.109.013, 2004.



**Radiocarbon analysis  
of elemental and  
organic carbon in  
Switzerland from  
2008–2012 – Part 1**

P. Zotter et al.

Title Page

Abstract

Introduction

Conclusions

References

Tables

Figures

◀

▶

◀

▶

Back

Close

Full Screen / Esc

Printer-friendly Version

Interactive Discussion

Gilardoni, S., Vignati, E., Cavalli, F., Putaud, J. P., Larsen, B. R., Karl, M., Stenström, K., Genberg, J., Henne, S., and Dentener, F.: Better constraints on sources of carbonaceous aerosols using a combined  $^{14}\text{C}$  – macro tracer analysis in a European rural background site, *Atmos. Chem. Phys.*, 11, 5685–5700, doi:10.5194/acp-11-5685-2011, 2011.

5 Glasius, M., la Cour, A., and Lohse, C.: Fossil and nonfossil carbon in fine particulate matter: a study of five European cities, *J. Geophys. Res.*, 116, D11302, doi:10.1029/2011JD015646, 2011.

Hallquist, M., Wenger, J. C., Baltensperger, U., Rudich, Y., Simpson, D., Claeys, M., Dommen, J., Donahue, N. M., George, C., Goldstein, A. H., Hamilton, J. F., Herrmann, H., Hoffmann, T., Iinuma, Y., Jang, M., Jenkin, M. E., Jimenez, J. L., Kiendler-Scharr, A., Maenhaut, W., McFiggans, G., Mentel, Th. F., Monod, A., Prévôt, A. S. H., Seinfeld, J. H., Surratt, J. D., Szmigielski, R., and Wildt, J.: The formation, properties and impact of secondary organic aerosol: current and emerging issues, *Atmos. Chem. Phys.*, 9, 5155–5236, doi:10.5194/acp-9-5155-2009, 2009.

15 Harrison, R. M., Beddows, D. C. S., Hu, L., and Yin, J.: Comparison of methods for evaluation of wood smoke and estimation of UK ambient concentrations, *Atmos. Chem. Phys.*, 12, 8271–8283, doi:10.5194/acp-12-8271-2012, 2012.

Heal, M. R.: The application of carbon-14 analyses to the source apportionment of atmospheric carbonaceous particulate matter: a review, *Anal. Bioanal. Chem.*, 406, 81–98, doi:10.1007/s00216-013-7404-1, 2014.

20 Hennigan, C. J., Miracolo, M. A., Engelhart, G. J., May, A. A., Presto, A. A., Lee, T., Sullivan, A. P., McMeeking, G. R., Coe, H., Wold, C. E., Hao, W.-M., Gilman, J. B., Kuster, W. C., de Gouw, J., Schichtel, B. A., J. L. Collett Jr., Kreidenweis, S. M., and Robinson, A. L.: Chemical and physical transformations of organic aerosol from the photo-oxidation of open biomass burning emissions in an environmental chamber, *Atmos. Chem. Phys.*, 11, 7669–7686, doi:10.5194/acp-11-7669-2011, 2011.

Herich, H., Hueglin, C., and Buchmann, B.: A 2.5 year's source apportionment study of black carbon from wood burning and fossil fuel combustion at urban and rural sites in Switzerland, *Atmos. Meas. Tech.*, 4, 1409–1420, doi:10.5194/amt-4-1409-2011, 2011.

30 Herich, H., Gianini, M. F. D., Piot, C., Moènik, G., Jaffrezo, J. L., Besombes, J. L., Prévôt, A. S. H., and Hueglin, C.: Overview of the impact of wood burning emissions on carbonaceous aerosols and PM in large parts of the Alpine region, *Atmos. Environ.*, 89, 64–75, doi:10.1016/j.atmosenv.2014.02.008, 2014.

## Radiocarbon analysis of elemental and organic carbon in Switzerland from 2008–2012 – Part 1

P. Zotter et al.

Title Page

Abstract

Introduction

Conclusions

References

Tables

Figures

◀

▶

◀

▶

Back

Close

Full Screen / Esc

Printer-friendly Version

Interactive Discussion

Heringa, M. F., DeCarlo, P. F., Chirico, R., Tritscher, T., Dommen, J., Weingartner, E., Richter, R., Wehrle, G., Prévôt, A. S. H., and Baltensperger, U.: Investigations of primary and secondary particulate matter of different wood combustion appliances with a high-resolution time-of-flight aerosol mass spectrometer, *Atmos. Chem. Phys.*, 11, 5945–5957, doi:10.5194/acp-11-5945-2011, 2011.

Hodzic, A., Jimenez, J. L., Prévôt, A. S. H., Szidat, S., Fast, J. D., and Madronich, S.: Can 3-D models explain the observed fractions of fossil and non-fossil carbon in and near Mexico City?, *Atmos. Chem. Phys.*, 10, 10997–11016, doi:10.5194/acp-10-10997-2010, 2010.

Huang, J., Kang, S., Shen, C., Cong, Z., Liu, K., Wang, W., and Liu, L.: Seasonal variations and sources of ambient fossil and biogenic-derived carbonaceous aerosols based on  $^{14}\text{C}$  measurements in Lhasa, Tibet, *Atmos. Res.*, 96, 553–559, doi:10.1016/j.atmosres.2010.01.003, 2010.

IPCC: Climate Change 2013: The Physical Science Basis, Contribution of Working Group I to the Fifth Assessment Report of the Intergovernmental Panel on Climate Change, edited by: Stocker, T. F., Qin, D., Plattner, G.-K., Tignor, M., Allen, S. K., Boschung, J., Nauels, A., Xia, Y., Bex, V., and Midgley, P. M., Cambridge University Press, Cambridge, UK and New York, NY, USA, 2013.

Jacobson, M. C., Hansson, H. C., Noone, K. J., and Charlson, R. J.: Organic atmospheric aerosols: review and state of the science, *Rev. Geophys.*, 38, 267–294, doi:10.1029/1998RG000045, 2000.

Jimenez, J. L., Canagaratna, M. R., Donahue, N. M., Prevot, A. S. H., Zhang, Q., Kroll, J. H., DeCarlo, P. F., Allan, J. D., Coe, H., Ng, N. L., Aiken, A. C., Docherty, K. S., Ulbrich, I. M., Grieshop, A. P., Robinson, A. L., Duplissy, J., Smith, J. D., Wilson, K. R., Lanz, V. A., Hueglin, C., Sun, Y. L., Tian, J., Laaksonen, A., Raatikainen, T., Rautiainen, J., Vaattovaara, P., Ehn, M., Kulmala, M., Tomlinson, J. M., Collins, D. R., Cubison, M. J., E, Dunlea, J., Huffman, J. A., Onasch, T. B., Alfarra, M. R., Williams, P. I., Bower, K., Kondo, Y., Schneider, J., Drewnick, F., Borrmann, S., Weimer, S., Demerjian, K., Salcedo, D., Cottrell, L., Griffin, R., Takami, A., Miyoshi, T., Hatakeyama, S., Shimono, A., Sun, J. Y., Zhang, Y. M., Dzepina, K., Kimmel, J. R., Sueper, D., Jayne, J. T., Herndon, S. C., Trimborn, A. M., Williams, L. R., Wood, E. C., Middlebrook, A. M., Kolb, C. E., Baltensperger, U., and Worsnop, D. R.: Evolution of organic aerosols in the atmosphere, *Science*, 326, 1525–1529, doi:10.1126/science.1180353, 2009.

**Radiocarbon analysis  
of elemental and  
organic carbon in  
Switzerland from  
2008–2012 – Part 1**

P. Zotter et al.

Title Page

Abstract

Introduction

Conclusions

References

Tables

Figures

◀

▶

◀

▶

Back

Close

Full Screen / Esc

Printer-friendly Version

Interactive Discussion

Johansson, L. S., Tullin, C., Leckner, B., and Sjövall, P.: Particle emissions from biomass combustion in small combustors, *Biomass Bioenerg.*, 25, 435–446, doi:10.1016/S0961-9534(03)00036-9, 2003.

Kessler, S. H., Smith, J. D., Che, D. L., Worsnop, D. R., Wilson, K. R., and Kroll, J. H.: Chemical sinks of organic aerosol: kinetics and products of the heterogeneous oxidation of erythritol and levoglucosan, *Environ. Sci. Technol.*, 44, 7005–7010, doi:10.1021/es101465m, 2010.

Khalil, M. A. K. and Rasmussen, R. A.: Tracers of wood smoke, *Atmos. Environ.*, 37, 1211–1222, doi:10.1016/S1352-2310(02)01014-2, 2003.

Lanz, V. A., Alfara, M. R., Baltensperger, U., Buchmann, B., Hueglin, C., Szidat, S., Wehrli, M. N., Wacker, L., Weimer, S., Caseiro, A., Puxbaum, H., and Prevot, A. S. H.: Source attribution of submicron organic aerosols during wintertime inversions by advanced factor analysis of aerosol mass spectra, *Environ. Sci. Technol.*, 42, 214–220, doi:10.1021/es0707207, 2008.

Lanz, V. A., Prévôt, A. S. H., Alfara, M. R., Weimer, S., Mohr, C., DeCarlo, P. F., Gianini, M. F. D., Hueglin, C., Schneider, J., Favez, O., D'Anna, B., George, C., and Baltensperger, U.: Characterization of aerosol chemical composition with aerosol mass spectrometry in Central Europe: an overview, *Atmos. Chem. Phys.*, 10, 10453–10471, doi:10.5194/acp-10-10453-2010, 2010.

Larsen, B. R., Gilardoni, S., Stenström, K., Niedzialek, J., Jimenez, J., and Belis, C. A.: Sources for PM air pollution in the Po Plain, Italy: II. Probabilistic uncertainty characterization and sensitivity analysis of secondary and primary sources, *Atmos. Environ.*, 50, 203–213, doi:10.1016/j.atmosenv.2011.12.038, 2012.

Lee, T., Sullivan, A. P., Mack, L., Jimenez, J. L., Kreidenweis, S. M., Onasch, T. B., Worsnop, D. R., Malm, W., Wold, C. E., Hao, W. M., and Collett, J. L.: Chemical smoke marker emissions during flaming and smoldering phases of laboratory open burning of wildland fuels, *Aerosol Sci. Tech.*, 44, I–V, doi:10.1080/02786826.2010.499884, 2010.

Levin, I., Naegler, T., Kromer, B., Diehl, M., Francey, R. J., Gomez-Pelaez, A. J., Steele, L. P., Wagenbach, D., Weller, R., and Worthy, D. E.: Observations and modelling of the global distribution and long-term trend of atmospheric  $^{14}\text{CO}_2$ , *Tellus B*, 62, 26–46, doi:10.1111/j.1600-0889.2009.00446.x, 2010.

Liu, D., Allan, J. D., Young, D. E., Coe, H., Beddows, D., Fleming, Z. L., Flynn, M. J., Gallagher, M. W., Harrison, R. M., Lee, J., Prévôt, A. H. S., Taylor, J. W., Yin, J., Williams, P.





## Radiocarbon analysis of elemental and organic carbon in Switzerland from 2008–2012 – Part 1

P. Zotter et al.

Title Page

Abstract

Introduction

Conclusions

References

Tables

Figures

◀

▶

◀

▶

Back

Close

Full Screen / Esc

Printer-friendly Version

Interactive Discussion

tative determination of wood burning and traffic emission contributions to particulate matter, *Environ. Sci. Technol.*, 42, 3316–3323, doi:10.1021/es702253m, 2008a.

Sandradewi, J., Prévôt, A. S. H., Alfarra, M. R., Szidat, S., Wehrl, M. N., Ruff, M., Weimer, S., Lanz, V. A., Weingartner, E., Perron, N., Caseiro, A., Kasper-Giebl, A., Puxbaum, H., Wacker, L., and Baltensperger, U.: Comparison of several wood smoke markers and source apportionment methods for wood burning particulate mass, *Atmos. Chem. Phys. Discuss.*, 8, 8091–8118, doi:10.5194/acpd-8-8091-2008, 2008b.

Schauer, J. J., Kleeman, M. J., Cass, G. R., and Simoneit, B. R. T.: Measurement of emissions from air pollution sources., 1. C1 through C29 organic compounds from meat charbroiling, *Environ. Sci. Technol.*, 33, 1566–1577, doi:10.1021/es980076j, 1999.

Schauer, J. J., Kleeman, M. J., Cass, G. R., and Simoneit, B. R. T.: Measurement of emissions from air pollution sources., 3. C1–C29 organic compounds from fireplace combustion of wood, *Environ. Sci. Technol.*, 35, 1716–1728, doi:10.1021/es001331e, 2001.

Schmid, H., Laskus, L., Abraham, H. J., Baltensperger, U., Lavanchy, V., Bizjak, M., Burba, P., Cachier, H., Crow, D., Chow, J., Gnauk, T., Even, A., ten Brink, H. M., Giesen, K.-P., Hitzenberger, R., Hueglin, C., Maenhaut, W., Pio, C., Carvalho, A., Putaud, J.-P., Toom-Saunty, D., and Puxbaum, H.: Results of the “carbon conference” international aerosol carbon round robin test stage I, *Atmos. Environ.*, 35, 2111–2121, 2001.

Schmidl, C., Marr, I. L., Caseiro, A., Kotianová, P., Berner, A., Bauer, H., Kasper-Giebl, A., and Puxbaum, H.: Chemical characterisation of fine particle emissions from wood stove combustion of common woods growing in mid-European Alpine regions, *Atmos. Environ.*, 42, 126–141, doi:10.1016/j.atmosenv.2007.09.028, 2008.

Schmidl, C., Lüsser, M., Padouvas, E., Lasselsberger, L., Rzáca, M., Ramirez-Santa Cruz, C., Handler, M., Peng, G., Bauer, H., and Puxbaum, H.: Particulate and gaseous emissions from manually and automatically fired small scale combustion systems, *Atmos. Environ.*, 45, 7443–7454, doi:10.1016/j.atmosenv.2011.05.006, 2011.

Steinbacher, M., Zellweger, C., Schwarzenbach, B., Bugmann, S., Buchmann, B., Ordóñez, C., Prevot, A. S. H., and Hueglin, C.: Nitrogen oxide measurements at rural sites in Switzerland: bias of conventional measurement techniques, *J. Geophys. Res.-Atmos.*, 112, D11307, doi:10.1029/2006JD007971, 2007.

Stuiver, M. and Polach, H. A.: Reporting of C-14 data – discussion, *Radiocarbon*, 19, 355–363, <https://journals.uair.arizona.edu/index.php/radiocarbon/article/view/493/498>, 1977.



**Radiocarbon analysis  
of elemental and  
organic carbon in  
Switzerland from  
2008–2012 – Part 1**

P. Zotter et al.

Title Page

Abstract

Introduction

Conclusions

References

Tables

Figures

◀

▶

◀

▶

Back

Close

Full Screen / Esc

Printer-friendly Version

Interactive Discussion

- Tanner, R. L., Parkhurst, W. J., and McNichol, A. P.: Fossil sources of ambient aerosol carbon based on  $^{14}\text{C}$  measurements, *Aerosol Sci. Tech.*, 38, 133–139, 2004.
- Turpin, B. J. and Lim, H. J.: Species contributions to  $\text{PM}_{2.5}$  mass concentrations: revisiting common assumptions for estimating organic mass, *Aerosol Sci. Tech.*, 35, 602–610, doi:10.1080/02786820152051454, 2001.
- Valmari, T., Kauppinen, E. I., Kurkela, J., Jokiniemi, J. K., Sfiris, G., and Revitzer, H.: Fly ash formation and deposition during fluidized bed combustion of willow, *J. Aerosol Sci.*, 29, 445–459, doi:10.1016/S0021-8502(97)10021-0, 1998.
- Viana, M., Chi, X., Maenhaut, W., Cafmeyer, J., Querol, X., Alastuey, A., Mikuška, P., and Večeřa, Z.: Influence of sampling artefacts on measured PM, OC, and EC levels in carbonaceous aerosols in an urban area, *Aerosol Sci. Tech.*, 40, 107–117, doi:10.1080/02786820500484388, 2006.
- Wacker, L., Christl, M., and Synal, H. A.: Bats: a new tool for AMS data reduction, *Nucl. Instrum. Meth. B*, 268, 976–979, doi:10.1016/j.nimb.2009.10.078, 2010.
- Wacker, L., Fahrni, S. M., Hajdas, I., Molnar, M., Synal, H. A., Szidat, S., and Zhang, Y. L.: A versatile gas interface for routine radiocarbon analysis with a gas ion source, *Nucl. Instrum. Meth. B*, 294, 315–319, doi:10.1016/j.nimb.2012.02.009, 2013.
- WHO: Air Quality Guidelines for Particulate Matter, Ozone, Nitrogen Dioxide and Sulfur Dioxide, Global Update 2005, Summary of Risk Assessment, World Health Organization, document WHO/SDE/PHE/OEH/06.02, Geneva, 2006.
- Zapf, A., Nesje, A., Szidat, S., Wacker, L., and Schwikowski, M.: C-14 measurements of ice samples from the Juvfonna ice tunnel, Jotunheimen, southern Norway-validation of a C-14 dating technique for glacier ice, *Radiocarbon*, 55, 571–578, doi:10.2458/azu\_js\_rc.55.16320, 2013.
- Zencak, Z., Elmquist, M., and Gustafsson, O.: Quantification and radiocarbon source apportionment of black carbon in atmospheric aerosols using the CTO-375 method, *Atmos. Environ.*, 41, 7895–7906, doi:10.1016/j.atmosenv.2007.06.006, 2007.
- Zhang, Y. L., Perron, N., Ciobanu, V. G., Zotter, P., Minguillón, M. C., Wacker, L., Prévôt, A. S. H., Baltensperger, U., and Szidat, S.: On the isolation of OC and EC and the optimal strategy of radiocarbon-based source apportionment of carbonaceous aerosols, *Atmos. Chem. Phys.*, 12, 10841–10856, doi:10.5194/acp-12-10841-2012, 2012.
- Zhang, Y. L., Li, J., Zhang, G., Zotter, P., Huang, R. J., Tang, J. H., Wacker, L., Prevot, A. S., and Szidat, S.: Radiocarbon-based source apportionment of carbonaceous aerosols at a re-

gional background site on hainan island, South China, Environ. Sci. Technol., 48, 2651–2659, doi:10.1021/es4050852, 2014.

- Zotter, P., Zhang, Y. L., El-Haddad, I., Ciobanu, V. G., Daellenbach, K. R., Salazar, G. A., Wacker, L., Herich, H., Hueglin, C., Baltensperger, U., Szidat, S., and Prévôt, A. H. S.:  
5 Radiocarbon analysis of elemental and organic carbon in Switzerland during winter-smog episodes from 2008 to 2012 – Part II: daily, seasonal and yearly variability, Atmos. Chem. Phys., in preparation, 2014.

**Radiocarbon analysis  
of elemental and  
organic carbon in  
Switzerland from  
2008–2012 – Part 1**

P. Zotter et al.

Title Page

Abstract

Introduction

Conclusions

References

Tables

Figures



Back

Close

Full Screen / Esc

Printer-friendly Version

Interactive Discussion



## Radiocarbon analysis of elemental and organic carbon in Switzerland from 2008–2012 – Part 1

P. Zotter et al.

Title Page

Abstract

Introduction

Conclusions

References

Tables

Figures

◀

▶

◀

▶

Back

Close

Full Screen / Esc

Printer-friendly Version

Interactive Discussion



**Table 1.** List of all stations, their classification according to the Swiss Federal Office for the Environment (BAFU), their general location in Switzerland, their coordinates and their abbreviations which are used later in the text, figures and tables.

Station name	Station code	General location	Station type	Altitude
Reiden-A2	REI	north of the Alps/Swiss Plateau	rural/highway	510 m
Basel-St. Johann	BAS		urban/background	308 m
Sissach-West	SIS		suburban/traffic	410 m
Solothurn-Altwyberhüsli	SOL		urban/background	502 m
Payerne	PAY		rural/background	539 m
Zürich-Kaserne	ZUR		urban/background	457 m
St. Gallen-Rorschacherstrasse	STG		urban/traffic	457 m
Bern-Bollwerk	BER		urban/traffic	506 m
Vaduz-Austrasse	VAD	north of the Alps/alpine valley	suburban/traffic	706 m
Massongex	MAS		rural/industry	452 m
Schächental	SCH		rural/background	995 m
Chiasso	CHI	south of the Alps	urban/traffic	291 m
Magadino-Cadenazzo	MAG		rural/background	254 m
Moleno-A2	MOL	south of the Alps/alpine valley	rural/highway	305 m
Roveredo-Stazione	ROV		suburban/background	370 m
San-Vittore	SVI		rural/traffic	330 m

## Radiocarbon analysis of elemental and organic carbon in Switzerland from 2008–2012 – Part 1

P. Zotter et al.

Title Page

Abstract

Introduction

Conclusions

References

Tables

Figures

◀

▶

◀

▶

Back

Close

Full Screen / Esc

Printer-friendly Version

Interactive Discussion



**Table 2.** Overview of all analysis carried out and which stations participated during which time period.

analysis	filter selection	Stations and time period
EC/OC concentrations	all samples ( $n = 320$ )	ZUR, PAY, MAG, SOL, SIS, STG, VAD, SVI and CHI (winter 2007/2008–2011/2012)
$^{14}\text{C}$ in EC and OC	all samples ( $n = 320 \times 2$ )	BER (winter 2008/2009–2012/2013), MAS (winter 2008/2009–2011/2012),
water-soluble ions	all samples ( $n = 320$ )	BAS (only winter 2007/2008–2008/2009), SCH (only winter 2010/2011),
levoglucosan	130 samples	REI, MOL and ROV (only winter 2007/2008), yearly cycle ZUR (Aug 2008–Jul 2009)



## Radiocarbon analysis of elemental and organic carbon in Switzerland from 2008–2012 – Part 1

P. Zotter et al.

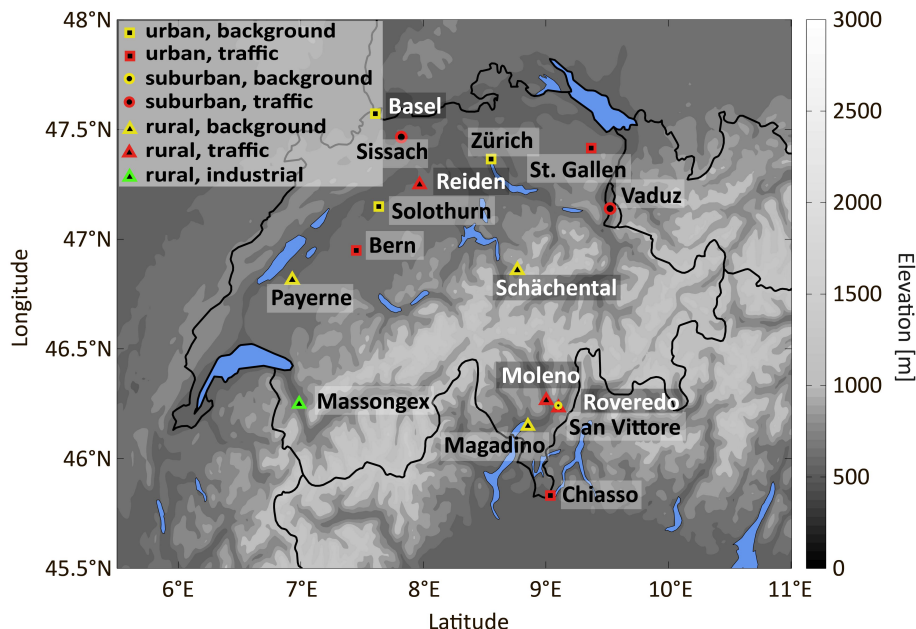


**Figure 1.** Location of the different stations in Switzerland investigated in this study. White labels indicate stations from which filters from only one or two winters were analyzed. For all other stations samples from four or five winters were studied.

Title Page	
Abstract	Introduction
Conclusions	References
Tables	Figures
◀	▶
◀	▶
Back	Close
Full Screen / Esc	
Printer-friendly Version	
Interactive Discussion	



## Radiocarbon analysis of elemental and organic carbon in Switzerland from 2008–2012 – Part 1

P. Zotter et al.

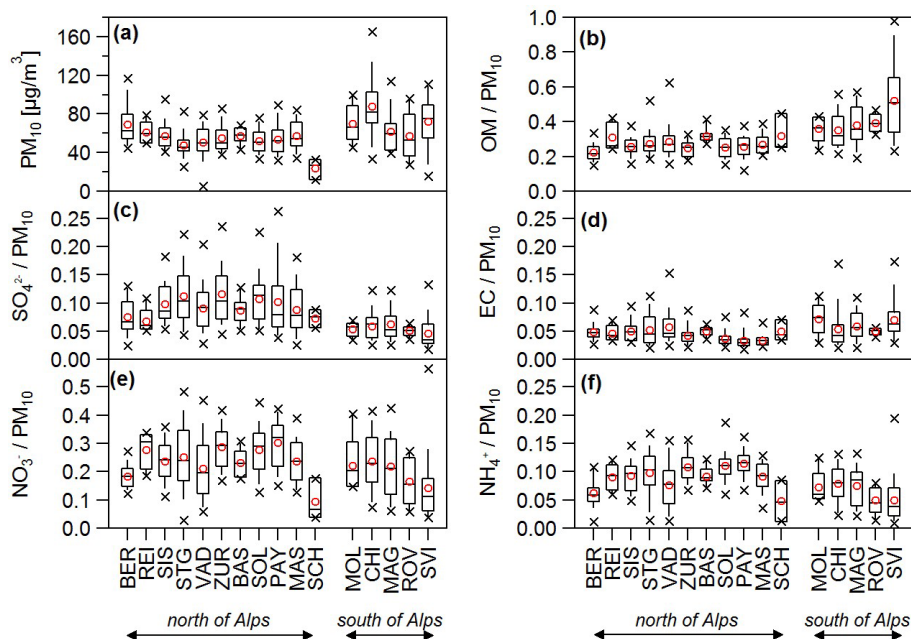


**Figure 2.** Whisker box plots of the fractional contributions of the major constituents of  $\text{PM}_{10}$  (water-soluble ions  $\text{NO}_3^-$ ,  $\text{SO}_4^{2-}$  and  $\text{NH}_4^+$  as well as EC and  $\text{OM} = \text{OC} \times 1.6$ ) from all analyzed winter samples ( $n \sim 300$ ). The open red circles represent the mean and the black crosses the max. and min. values. The boxes represent the 25th (lower line), 50th (middle line) and 75th (top line) percentiles. The end of the vertical bars denote the 10th (below the box) and 90th (above the box) percentiles. Stations north and south of the Alps are sorted from the left to the right from the nominal most traffic-influenced station (see Table 1) to the most rural one. Data from the yearly cycle in ZUR are excluded. The Whisker box plots showing the absolute concentrations are presented in Fig. S3 in the Supplement.

**Radiocarbon analysis of elemental and organic carbon in Switzerland from 2008–2012 – Part 1**

P. Zotter et al.

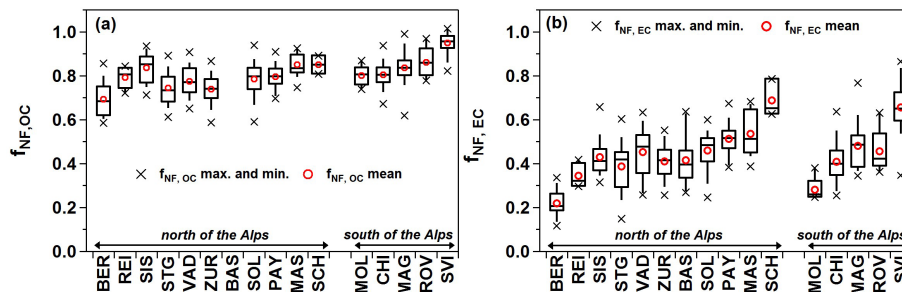


**Figure 3.** Whisker box plots of the fractional non-fossil contributions of OC (a) and EC (b) summarizing all winter filter samples measured for  $^{14}\text{C}$  ( $n \sim 300$  for OC and EC). Stations north and south of the Alps are sorted from the left to the right from the nominal most traffic-influenced station (see Table 1) to the most rural one.  $f_{NF,OC}$  values for BAS are not included since several values above one were found (see Sect. 3.2). Data from the yearly cycle in ZUR are excluded as well.

Title Page

Abstract

Introduction

Conclusions

References

Tables

Figures

◀

▶

◀

▶

Back

Close

Full Screen / Esc

Printer-friendly Version

Interactive Discussion



**Radiocarbon analysis of elemental and organic carbon in Switzerland from 2008–2012 – Part 1**

P. Zotter et al.

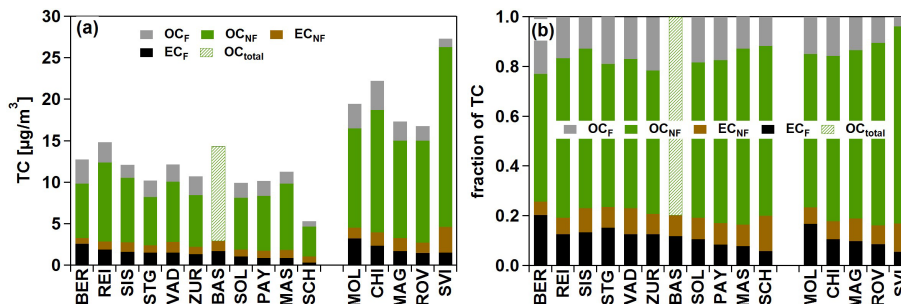


**Figure 4.** Average over all analyzed winter samples ( $n \sim 300$ ) for each station of  $\text{EC}_F$ ,  $\text{EC}_{NF}$ ,  $\text{OC}_{NF}$  and  $\text{OC}_F$  (a) as well as their relative contribution to TC (b). Total OC is displayed for BAS since  $f_{NF,OC}$  values for this station are not included in the analysis due to several values above one (see Sect. 3.2.1). Data from the yearly cycle in ZUR are excluded as well.

Title Page	
Abstract	Introduction
Conclusions	References
Tables	Figures
◀	▶
◀	▶
Back	Close
Full Screen / Esc	
Printer-friendly Version	
Interactive Discussion	



## Radiocarbon analysis of elemental and organic carbon in Switzerland from 2008–2012 – Part 1

P. Zotter et al.

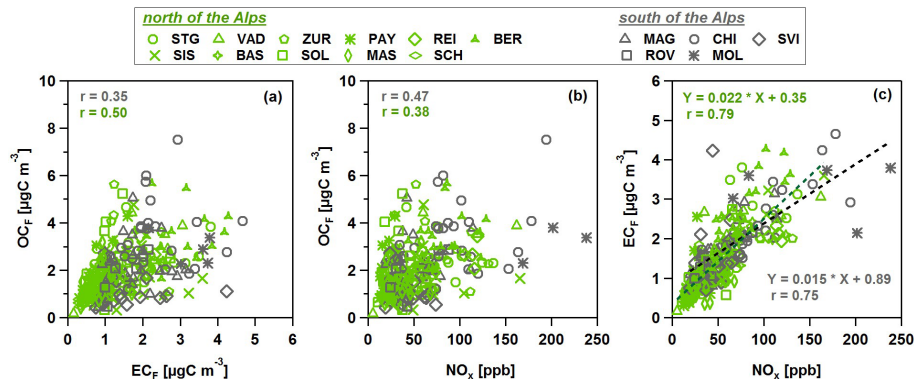


**Figure 5.** Comparison for stations north and south of the Alps for **(a)**  $EC_F$  and  $OC_F$ , **(b)**  $NO_x$  and  $OC_F$  as well as **(c)**  $NO_x$  and  $EC_F$ .  $OC_F$  values from BAS and all data from the yearly cycle in ZUR are excluded (see Sects. 3.2.1 and 1). An orthogonal distance regression was used to fit the data.

## Radiocarbon analysis of elemental and organic carbon in Switzerland from 2008–2012 – Part 1

P. Zotter et al.

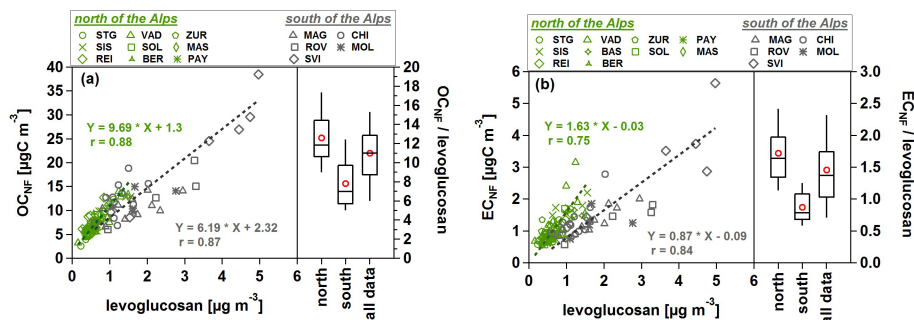


**Figure 6.** Scatter plot of  $OC_{NF}$  (a) and  $EC_{NF}$  (b) vs. levoglucosan combined with Whisker box plots of their ratios for all measured winter samples (red circles denote the mean).  $OC_{NF}$  values from BAS and all data from the yearly cycle in ZUR are excluded (see Sects. 3.2.1 and 1). Levoglucosan data is only available for the first two winter seasons (see Table 2). An orthogonal distance regression was used to fit the data.

Title Page

Abstract

Introduction

Conclusions

References

Tables

Figures

◀

▶

◀

▶

Back

Close

Full Screen / Esc

Printer-friendly Version

Interactive Discussion

## Radiocarbon analysis of elemental and organic carbon in Switzerland from 2008–2012 – Part 1

P. Zotter et al.

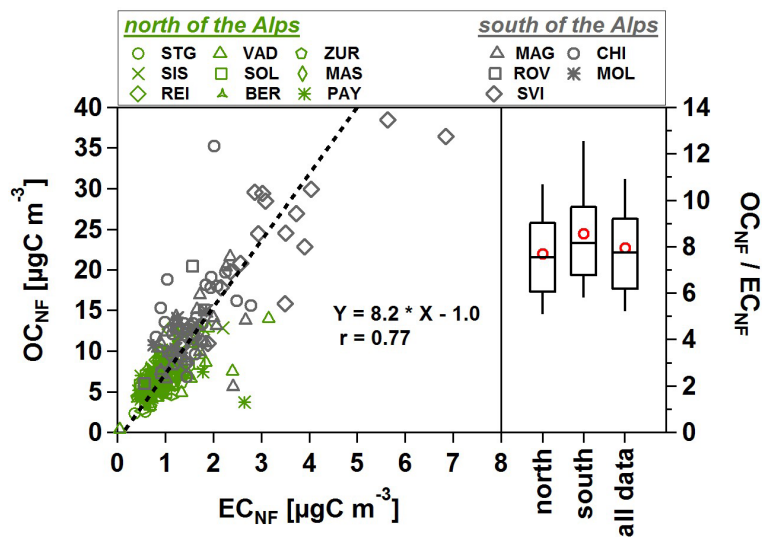


**Figure 7.** Comparison of OC<sub>NF</sub> and EC<sub>NF</sub> combined with Whisker box plots of their ratios for all measured winter samples (red circles denote the mean). OC<sub>NF</sub> values from BAS and all data from the yearly cycle in ZUR are excluded (see Sects. 3.2.1 and 1). An orthogonal distance regression was used to fit the data.

**Radiocarbon analysis of elemental and organic carbon in Switzerland from 2008–2012 – Part 1**

P. Zotter et al.

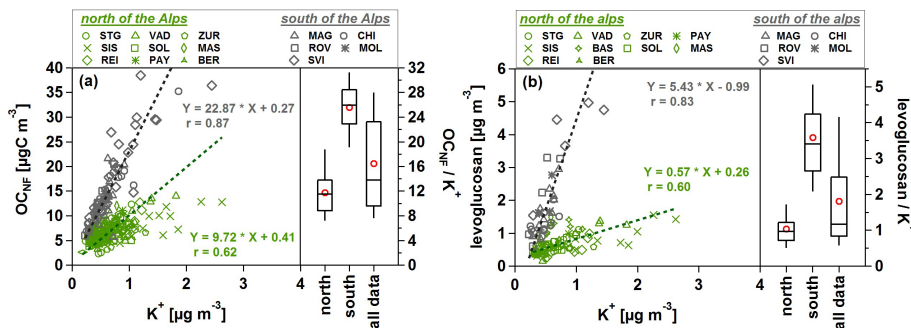


**Figure 8.**  $OC_{NF}$  (a) and levoglucosan (b) as a function of the  $K^+$  concentrations combined with Whisker box plots of their ratios for all measured winter samples (red circles denote the mean).  $OC_{NF}$  values from BAS and all data from the yearly cycle in ZUR are excluded (see Sects. 3.2.1 and 1). Levoglucosan data is only available for the first 2 winter seasons (see Table 2). An orthogonal distance regression was used to fit the data.

Title Page

Abstract Introduction

Conclusions References

Tables Figures

◀ ▶

◀ ▶

Back Close

Full Screen / Esc

Printer-friendly Version

Interactive Discussion

